

Field-Circuit Coupled Models in Electromagnetic Simulation*

Herbert De Gersem^{a,†}, Kay Hameyer^b, Thomas Weiland^a

^a Technische Universität Darmstadt, Computational Electromagnetics Laboratory (TEMF), Schloßgartenstraße 8, D-64289 Darmstadt, Germany

^b Katholieke Universiteit Leuven, Dep. ESAT, Div. ELECTA, Kasteelpark Arenberg 10, B-3001 Leuven-Heverlee, Belgium

Abstract

A general field-circuit coupling mechanism for electromagnetic models is presented. The topological treatment of the circuit allows for a well-defined choice of coupling unknowns and equations, both for couplings of magnetic fields to magnetic circuits and couplings of magnetic fields to electric circuits. The properties of the resulting systems of equations are studied and appropriate iterative solution techniques are proposed. Two technical examples demonstrate the modelling flexibility provided by field-circuit coupling.

Keywords: Coupled Problems, Electromagnetic Simulation

1 Introduction

Circuit simulation is close to technical understanding, offers fast models, but requires skilled engineers to derive appropriate lumped parameters for insertion in the circuit model. A simulation approach based on a discretisation technique is more suited for models with arbitrary geometries and complicated excitations, is commonly automated up to a certain extent, but may require a considerable computational effort. For many electrotechnical problems, a circuit model may provide a sufficient accuracy for a part of the model whereas the remaining part requires a 2D or 3D discretisation, e.g. by the finite element (FE) method (Fig. 1). In that case, hybrid field-circuit coupled models offer an optimal trade-off between simulation accuracy and problem size. They require less simulation time compared to fully discretised models. Moreover, the presence of technical values such as voltages and currents triggers the engineer's experience and may help to detect conceptual and modelling faults at an early stage of the design.

The paper is organised as follows. Section 2 describes the topological treatment of the circuit model part. In Section 3 and Section 4, a magnetic FE model is coupled to a magnetic circuit and an electric circuit respectively. Section 5 discusses appropriate iterative solution techniques for the coupled systems of equations and Section 6 illustrates the coupling approaches for two electrotechnical devices.

*Herbert De Gersem is working in the cooperation project “DA-WE1 (TEMF/GSI)” with the “Gesellschaft für Schwerionenforschung (GSI)”, Darmstadt.

†Corresponding author. E-mail: degersem@temf.tu-darmstadt.de.

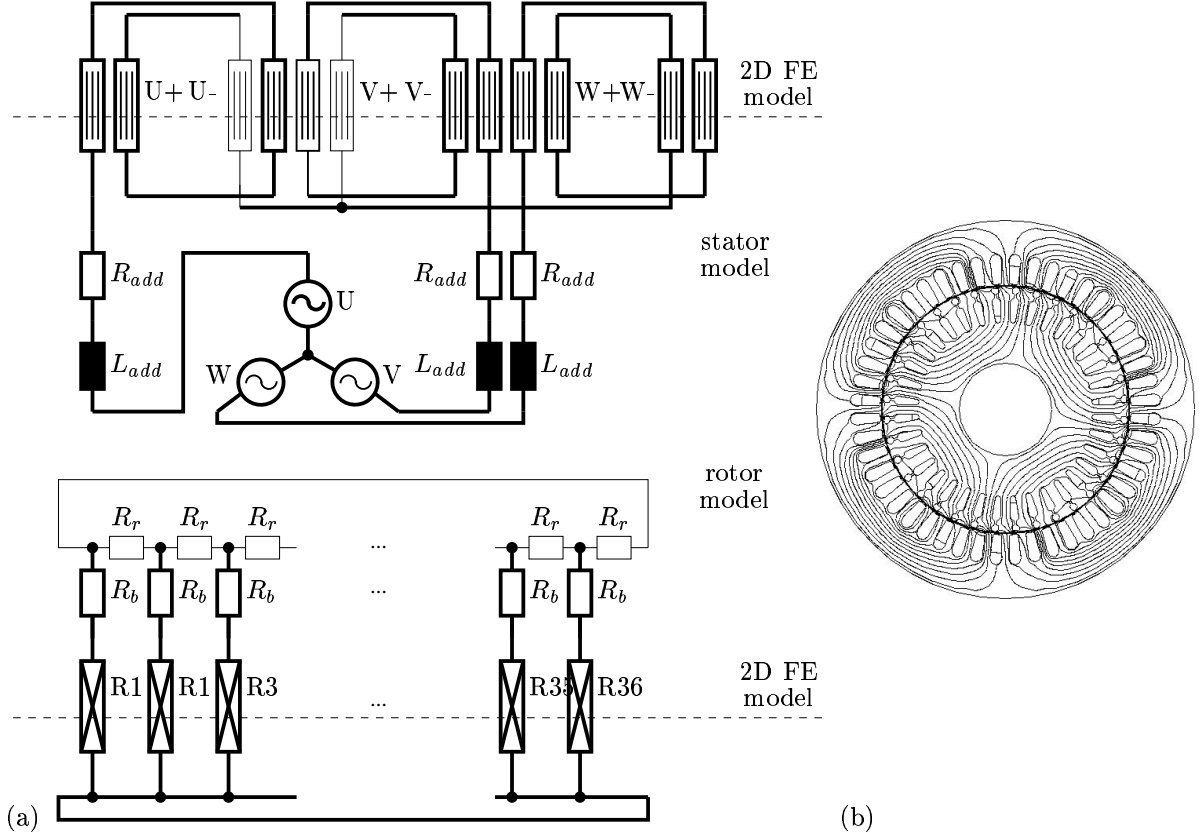


Figure 1: Three-phase induction machine model: (a) external electric circuit (thick and thin lines indicate twigs and links respectively) and (b) magnetic flux lines in the 2D FE model part.

2 Topological Circuit Model

We consider circuits which may consist of several disconnected parts and contain elements which are coupled through a FE model (Fig. 1a). A *loop* is a closed path through the circuit [1]. A *cut-set* is defined as a set of branches which upon removal would cause the number of disconnected circuit parts to increase by 1. A *tree* is a set of branches connecting all circuit nodes without forming loops. Tracing a tree through the circuit is done by selecting branches following a priority rule which will be defined below. The tree branches are called *twigs*, the remaining branches are called *links* and form the *co-tree*. A *fundamental cut-set* is formed by 1 twig and the unique set of links completing the cut-set. A *fundamental loop* consists of 1 link and the unique path through the tree closing the loop. The fundamental cut-sets and loops form maximal independent sets for the cut-sets and loops of the circuit respectively. The tree partitioning is algebraically represented by the *fundamental cut-set matrix* D and the *fundamental loop matrix* B containing the signed incidences of the circuit branches to the fundamental cut-sets and loops respectively. When the twigs are ordered first, the fundamental incidences matrices have the form

$$D = [I \quad D_{tw,ln}] , \quad (2.1)$$

$$B = [B_{ln,tw} \quad I] , \quad (2.2)$$

where the subscripts "tw" and "ln" indicate twigs and links or the associated fundamental cut-sets of loops respectively. A fundamental property of circuit theory is the relation $B_{ln,tw} =$

$-D_{\text{tw},\ln}^T$ [1]. Applying the Kirchhoff current law (KCL) and the Kirchhoff voltage law (KVL) to the fundamental cut-sets and loops respectively results in the expressions

$$[I \quad D_{\text{tw},\ln}] \begin{bmatrix} \underline{I}_{\text{tw}} \\ \underline{I}_{\ln} \end{bmatrix} = \begin{bmatrix} 0 \\ 0 \end{bmatrix}, \quad (2.3)$$

$$[B_{\ln,\text{tw}} \quad I] \begin{bmatrix} \Delta\underline{V}_{\text{tw}} \\ \Delta\underline{V}_{\ln} \end{bmatrix} = \begin{bmatrix} 0 \\ 0 \end{bmatrix}, \quad (2.4)$$

with \underline{I} and $\Delta\underline{V}$ denoting currents and voltage drops. Because the fundamental cut-sets and fundamental loops form linear independent sets, the relations in (2.3) and (2.4) are not over-determined as would be the case if a Tableau analysis would be applied. The circuit theory recalled here, does not restrict to electrical circuits. It can also be applied to e.g. magnetic and thermal circuits.

Five categories of circuit branches are distinguished based on the form of the relation between the voltage drop and the current of the branch:

- For an *independent voltage source*, the voltage drop is known a priori.
- For a *voltage-driven branch*, it is possible to express the voltage-current relation by

$$\underline{I}_{\text{br}} = G_{\text{br}}\Delta\underline{V}_{\text{br}} + \underline{f}_{\text{br,coup}} \quad (2.5)$$

where G_{br} is the DC conductance of the branch and $\underline{f}_{\text{br,coup}}$ is a coupling term.

- For a *voltage/current-driven branch*, both expressions (2.5) and (2.6) are applicable.
- For a *current-driven branch*, the voltage-current relation is of the form

$$\Delta\underline{V}_{\text{br}} = R_{\text{br}}\underline{I}_{\text{br}} + \underline{f}_{\text{br,coup}} \quad (2.6)$$

with R_{br} the DC resistance of the branch.

- For an *independent current source*, the current is known.

Branches are selected to participate to the tree in the order of priority indicated by the list above. To each circuit part, the following procedure is applied. The *set of connected nodes* collects all nodes that are already connected by the tree tracing procedure and initially consists of one arbitrarily chosen node. The *set of adjacent branches* contains all branches of which one vertex is connected. The tree is constructed by successively selecting the adjacent branch with the highest priority. The new twig is removed from the set of adjacent branches and its node that was not yet connected, is added to the set of connected nodes. Adjacent branches which are incident to this node, are removed from the set of adjacent branches whereas other branches incident to this node have to be removed. By construction, the priority of a twig is greater or equal to the priority of all links belonging to the associated fundamental cut-set. Similarly, the priority of a link is less or equal to the priorities of the twigs of the corresponding fundamental loop. This procedure favours voltage-driven branches and current-driven branches to be selected as twigs and links respectively. Voltage/current-driven branches take over the properties of voltage-driven branches or current-driven branches depending whether they are selected for the tree or the co-tree respectively. The exceptional cases when independent voltage and current sources show up in the co-tree and the tree respectively, deserve a special treatment. If an independent voltage source appears in the co-tree, the corresponding fundamental loop only contains independent voltage sources. If the KVL is satisfied for this loop, the independent-voltage-source link can be

omitted. Otherwise, the circuit problem has no solution. An analogous reasoning applies to the cut-set associated with an independent-current-source twig.

The circuit branches are indexed and sorted in the following order: independent-voltage-source twigs (subscript "twv"), voltage-driven twigs (subscript "two"), current-driven twigs (subscript "twu"), voltage-driven links (subscript "lnu"), current-driven links (subscript "lno") and independent-current-source links (subscript "lni"). The fundamental cut-set and loop matrices are partitioned accordingly:

$$D = \begin{bmatrix} I & 0 & 0 & D_{\text{twv},\text{lnu}} & D_{\text{twv},\text{lno}} & D_{\text{twv},\text{lni}} \\ 0 & I & 0 & D_{\text{two},\text{lnu}} & D_{\text{two},\text{lno}} & D_{\text{two},\text{lni}} \\ 0 & 0 & I & 0 & D_{\text{twu},\text{lno}} & D_{\text{twu},\text{lni}} \end{bmatrix}; \quad (2.7)$$

$$B = \begin{bmatrix} B_{\text{lnu},\text{twv}} & B_{\text{lnu},\text{two}} & 0 & I & 0 & 0 \\ B_{\text{lno},\text{twv}} & B_{\text{lno},\text{two}} & B_{\text{lno},\text{twu}} & 0 & I & 0 \\ B_{\text{lni},\text{twv}} & B_{\text{lni},\text{two}} & B_{\text{lni},\text{twu}} & 0 & 0 & I \end{bmatrix}. \quad (2.8)$$

The zero entries at position (3, 4) in D and (1, 3) in B are due to the application of the priority rules. A fundamental cutset associated with a current-driven twig can not contain voltage-driven branches because these have a higher priority. The symmetry property of the fundamental cut-set and loop matrices carries over to their subblocks: $B_{a,b} = -D_{b,a}^T$ for each subscript a and b .

The known voltage drops and known currents of the independent sources are collected in the vectors $\underline{\Delta V}_{\text{twv}}$ and $\underline{I}_{\text{lni}}$ respectively. The voltage-current relations are based on the positive-definite diagonal matrices G_{two} , G_{lnu} , R_{twu} , R_{lno} and the coupling terms $\underline{q}_{\text{two,coup}}$, $\underline{q}_{\text{lnu,coup}}$, $\underline{p}_{\text{twu,coup}}$ and $\underline{p}_{\text{lno,coup}}$. Two sets of unknowns are introduced: the voltage drops $\underline{\Delta V}_{\text{two}}$ along the voltage-driven twigs and the currents $\underline{I}_{\text{lno}}$ through the current-driven links. The currents through the current-driven twigs are

$$\underline{I}_{\text{twu}} = -D_{\text{twu},\text{lno}}\underline{I}_{\text{lno}} - D_{\text{twu},\text{lni}}\underline{I}_{\text{lni}} \quad (2.9)$$

whereas the voltage drops along the voltage-driven links are

$$\underline{\Delta V}_{\text{lnu}} = -B_{\text{lnu},\text{two}}\underline{\Delta V}_{\text{two}} - B_{\text{lnu},\text{twv}}\underline{\Delta V}_{\text{twv}}. \quad (2.10)$$

The expressions (2.5), (2.6), (2.9) and (2.10) are substituted into (2.3) and (2.4) yielding a mixed formulation for the circuit problem:

$$\begin{bmatrix} G_{\text{two}}^* & D_{\text{two},\text{lno}} \\ -B_{\text{lno},\text{two}} & -R_{\text{lno}}^* \end{bmatrix} \begin{bmatrix} \underline{\Delta V}_{\text{two}} \\ \underline{I}_{\text{lno}} \end{bmatrix} + \begin{bmatrix} \underline{q}_{\text{two,coup}}^* \\ \underline{p}_{\text{lno,coup}}^* \end{bmatrix} = \begin{bmatrix} -\underline{I}_{\text{two,src}} \\ \underline{\Delta V}_{\text{lno,src}} \end{bmatrix}, \quad (2.11)$$

with the positive-definite Schur complements

$$G_{\text{two}}^* = G_{\text{two}} - D_{\text{two},\text{lnu}}G_{\text{lnu}}B_{\text{lnu},\text{two}}, \quad (2.12)$$

$$R_{\text{lno}}^* = R_{\text{lno}} - B_{\text{lno},\text{twu}}R_{\text{twu}}D_{\text{twu},\text{lno}}, \quad (2.13)$$

the coupling terms

$$\underline{q}_{\text{two,coup}}^* = \underline{q}_{\text{two,coup}} - D_{\text{two},\text{lnu}}\underline{q}_{\text{lnu,coup}}, \quad (2.14)$$

$$\underline{p}_{\text{lno,coup}}^* = \underline{p}_{\text{lno,coup}} - B_{\text{lno},\text{twu}}\underline{p}_{\text{twu,coup}} \quad (2.15)$$

and the source terms

$$\underline{I}_{\text{two,src}} = D_{\text{two},\text{lni}}\underline{I}_{\text{lni}} - D_{\text{two},\text{lnu}}G_{\text{lnu}}B_{\text{lnu},\text{twv}}\underline{\Delta V}_{\text{twv}}; \quad (2.16)$$

$$\underline{\Delta V}_{\text{lno,src}} = B_{\text{lno},\text{twv}}\underline{\Delta V}_{\text{twv}} - B_{\text{lno},\text{twu}}R_{\text{twu}}D_{\text{twu},\text{lni}}\underline{I}_{\text{lni}}. \quad (2.17)$$

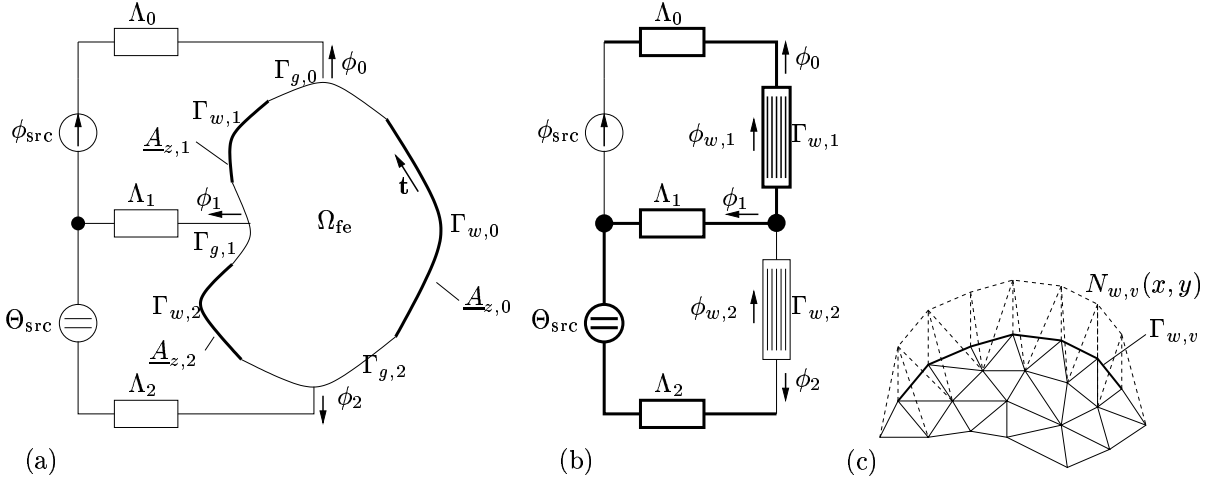


Figure 2: (a) Magnetic-field, magnetic-circuit coupled model, (b) circuit representation and (c) flux wall FE shape function.

The symmetry of the system (2.11) follows from the property $B_{a,b} = -D_{b,a}^T$. The spectrum of the system contains n_{two} positive eigenvalues and n_{lno} negative eigenvalues with n_{two} the number of voltage-driven twigs and n_{lno} the number of current-driven links.

3 Magnetic-Field, Magnetic-Circuit Coupling

The field-circuit coupling mechanisms are explained for 2D time-harmonic magnetodynamic FE models. The generalisation of the field-circuit coupling approach, to electrokinetic, transient and 3D models, is straightforward [2, 3, 4]. The governing partial differential equation (PDE) is

$$-\frac{\partial}{\partial x} \left(\nu \frac{\partial \underline{A}_z}{\partial x} \right) - \frac{\partial}{\partial y} \left(\nu \frac{\partial \underline{A}_z}{\partial y} \right) + j\omega\sigma \underline{A}_z = \frac{\sigma}{\ell_z} \Delta \underline{V} \quad (3.18)$$

with \underline{A}_z the phasor of the z -component of the magnetic vector potential \mathbf{A} , ω the pulsation, ν the reluctivity, σ the conductivity, $\Delta \underline{V}$ the voltage drop between the front and the rear of the model and ℓ_z the length of the model. Consider the 2D computational domain Ω_{fe} of Fig. 2a. The boundary $\partial\Omega$ is subdivided into *flux walls* $\Gamma_{w,p}$ and *flux gates* $\Gamma_{g,p}$, alternating along $\partial\Omega$ and ordered counter-clockwise. The magnetic vector potential is unknown but constant at each flux wall and is called a *floating potential*. The geometry of the device is triangulated. The linear FE shape functions associated with the mesh nodes are denoted by N_i and N_j . The floating potential constraints are enforced in the FE model by *flux wall shape functions* N_p and N_q obtained by gluing together the individual FE functions associated with all mesh vertices at $\Gamma_{w,p}$ (Fig. 2c). At a flux gate, homogeneous Neumann constraints are applied. The magnetic flux through the gate $\Gamma_{g,p}$ equals the difference of the floating potentials at the neighbouring flux walls multiplied by the length of the model:

$$\underline{I}_p = \ell_z (\underline{A}_{z,p+1} - \underline{A}_{z,p}) . \quad (3.19)$$

The flux wall $\Gamma_{w,0}$ is chosen as reference flux wall and gets a zero potential value. Applying the Galerkin procedure to (3.18) with the test and trial functions $\{N_i, N_p\}$ and $\{N_j, N_q\}$ results in the algebraic system of equations

$$\begin{bmatrix} K_{i,j} & K_{i,q} \\ K_{p,j} & K_{p,q} \end{bmatrix} \begin{bmatrix} \underline{u}_j \\ \underline{u}_q \end{bmatrix} + \begin{bmatrix} 0 \\ \underline{g}_p \end{bmatrix} = \begin{bmatrix} \underline{f}_i \\ \underline{f}_p \end{bmatrix} \quad (3.20)$$

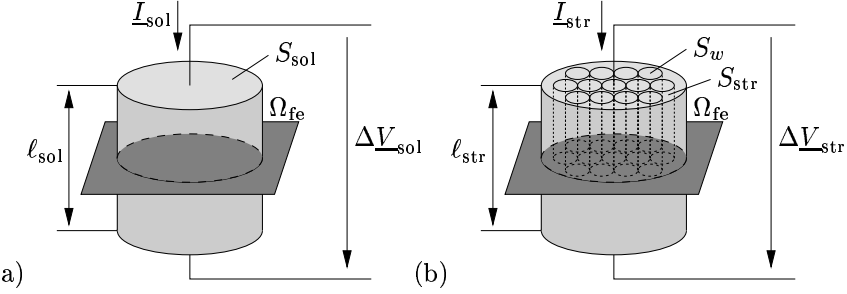


Figure 3: (a) Solid conductor model and (b) stranded conductor model.

with \underline{u}_j and \underline{u}_q the FE degrees of freedom associated with the standard FE shape functions and the flux wall shape functions respectively. The entries of the stiffness matrix K , the load vector \underline{f} and the unknown boundary integral \underline{g}_p are given by

$$K_{a,b} = \int_{\Omega_{fe}} \left(\nu \frac{\partial N_a}{\partial x} \frac{\partial N_b}{\partial x} + \nu \frac{\partial N_a}{\partial y} \frac{\partial N_b}{\partial y} + j\omega\sigma N_a N_b \right) d\Omega , \quad (3.21)$$

$$\underline{f}_a = \int_{\Omega_{fe}} \frac{\sigma}{\ell_z} \Delta V d\Omega , \quad (3.22)$$

$$\underline{g}_p = \int_{\Gamma_{w,p}} \left(-\nu \frac{\partial A_z}{\partial n} \right) N_p d\Gamma , \quad (3.23)$$

with $\partial/\partial n$ the derivation along the normal vector at $\Gamma_{w,p}$ outward with respect to Ω_{fe} . The terms \underline{g}_p correspond to the magnetic voltage drops between the two flux gates $\Gamma_{g,p}$ and $\Gamma_{g,p-1}$. If $\underline{g}_p = 0$, the magnetic flux can freely leave the FE model. This situation corresponds to FE models of which the flux gates are connected to each other by an infinitely permeable material. It is possible to describe the closing of the flux outside Ω_{fe} by connecting the FE model to an external magnetic equivalent circuit [5, 6]. The magnetic circuit is partitioned using the following priorities for twigs: magnetic voltage sources, magnetic reluctances, magnetic flux walls and magnetic flux sources (Fig. 2b). The coupled system of equations is

$$\begin{bmatrix} \chi_{mec} K_{i,j} & \chi_{mec} K_{i,lno} & 0 \\ \chi_{mec} K_{lno,j} & \chi_{mec} K_{lno,lno} + R_{lno} & B_{lno,two} \\ 0 & -D_{two,lno} & -G_{two} \end{bmatrix} \begin{bmatrix} \underline{I}_j \\ \underline{I}_{lno} \\ \Delta V_{two} \end{bmatrix} = \begin{bmatrix} \chi_{mec} f_i \\ \chi_{mec} f_p - \underline{I}_{lno,src} \\ \Delta V_{two,src} \end{bmatrix} . \quad (3.24)$$

The FE system part is scaled by $\chi_{mec} = 1/\ell_z$ in order to preserve the symmetry of the system. For convenience, flux-like quantities $\underline{I}_j = \ell_z \underline{u}_j$ are used as unknowns. The term $\chi_{mec} K_{lno,lno}$ represents the contribution of the FE model part to the magnetic reluctance of the fundamental loops whereas R_{lno} represents the contribution of the external reluctances. Schur complements are required if flux walls appear in the tree. These are not considered in (3.24) but follow the description of Section 2.

4 Magnetic-Field, Electric-Circuit Coupling

Electric-circuit, magnetic-field coupled models are the most frequently used field-circuit coupled models in the simulation of electrical energy transducers [7]. Two types of magnetically coupled circuit branches are considered (Fig. 3):

- Eddy current effects in massive conductors are resolved by the *solid conductor model*. The total current through the conductor is

$$\underline{I}_{\text{sol}} = G_{\text{sol}} \Delta \underline{V}_{\text{sol}} - \int_{\Omega_{\text{sol}}} j\omega \sigma \underline{A}_z d\Omega \quad (4.25)$$

with G_{sol} the DC conductance of the massive conductor, $\Delta \underline{V}_{\text{sol}}$ the voltage drop along the conductor and Ω_{sol} the cross-section of the conductor with the FE model. The expression (4.25) is of the form (2.5), hence, a solid conductor behaves as a voltage-driven circuit element.

- In many technical windings, the redistribution of the electric current can be neglected. The *stranded conductor model* is based on the assumption of a homogeneous distribution of the current density:

$$\underline{J}_{\text{str}} = \frac{N_{\text{str}}}{S_{\text{str}}} \underline{I}_{\text{str}} \quad \text{in } \Omega_{\text{str}} \quad (4.26)$$

with N_{str} the number of turns, S_{str} the area of the cross-section Ω_{str} of the winding with the FE model and $\underline{I}_{\text{str}}$ the applied current. The voltage drop along the winding is

$$\Delta \underline{V}_{\text{str}} = R_{\text{str}} \underline{I}_{\text{str}} + \frac{N_{\text{str}}}{S_{\text{str}}} \int_{\Omega_{\text{str}}} j\omega \underline{A}_z d\Omega \quad (4.27)$$

with R_{str} the DC resistance of the winding. Expression (4.27) reveals that the stranded conductor model has to be treated as a current-driven branch in the electric circuit.

The coupled system of equations reads

$$\begin{bmatrix} K_{\text{fe}} & Q_{\text{fe,two}} & P_{\text{fe,lno}} \\ Q_{\text{fe,two}}^T & \chi_{\text{ext}} G_{\text{two}} & \chi_{\text{ext}} D_{\text{two,lno}} \\ P_{\text{fe,lno}}^T & -\chi_{\text{ext}} B_{\text{lno,two}} & -\chi_{\text{ext}} R_{\text{lno}} \end{bmatrix} \begin{bmatrix} \underline{u}_{\text{fe}} \\ \Delta \underline{V}_{\text{two}} \\ \underline{I}_{\text{lno}} \end{bmatrix} = \begin{bmatrix} f_{\text{fe}} \\ \chi_{\text{ext}} \underline{I}_{\text{two,src}} \\ -\chi_{\text{ext}} \Delta \underline{V}_{\text{lno,src}} \end{bmatrix}. \quad (4.28)$$

with the factor $\chi_{\text{ext}} = 1/j\omega \ell_z$ symmetrising the coupled system. The entries of the discretised coupling terms $Q_{\text{fe,two}}$ and $P_{\text{fe,lno}}$ are given by

$$Q_{i,\text{sol}} = - \int_{\Omega_{\text{sol}}} \frac{\sigma}{\ell_z} N_i d\Omega; \quad (4.29)$$

$$P_{i,\text{str}} = - \int_{\Omega_{\text{str}}} \frac{N_{\text{str}}}{S_{\text{str}}} N_i d\Omega. \quad (4.30)$$

Solid-conductor links and stranded-conductor twigs are resolved by Schur complements as described in Section 2.

5 Solving Field-Circuit Coupled Systems

Since the dynamic interaction between electric and magnetic fields is of a linear nature, embedding both phenomena in one coupled system matrix is particularly attractive. The choice of the electromagnetic field and circuit unknowns influences the matrix structure and hence the memory and CPU requirements of iterative methods applied to solve the coupled systems of equations. Field-circuit coupled approaches can be interpreted as hybrid domain decomposition techniques coupling finite element discretisations to lower-dimensional circuit models. In some

Table 1: Properties of the circuit of the three-phase induction machine model.

number of branches	192
number of circuit nodes	155
number of connected circuit parts	2
number of tree branches	153
number of links	39
number of cutset equations	146
number of loop equations	2
number of circuit equations	148

cases, using a mixed formulation in terms of both current and voltage unknowns for the electrical circuit is recommended in order to preserve the sparsity of the system matrices.

The field-circuit coupling mechanism is designed in such a way that, as much as possible, the properties of the original FE part of the matrix are preserved. A few, relatively dense equations modelling the circuit are added to the FE system matrix. In case of time-harmonic simulation, the FE system part is complex symmetric, in case of transient simulation, symmetric and positive definite. The coupled system preserves symmetry, but not the positive definiteness. The coupled systems of equations are solved by Krylov subspace solvers for symmetric indefinite systems of equations. The transient system is solved by the Minimal Residual (MINRES) method [8] whereas the complex-symmetric time-harmonic system is solved by the Quasi-Minimal Residual (QMR) method [9]. Block variants of common stationary iterative methods such as Jacobi (JAC), Gauss-Seidel (GS) and Symmetric Successive Over-Relaxation (SSOR) are used to precondition the coupled systems of equations. Within each block, a preconditioner tuned to the particular part of the problem can be applied.

In the case of transient simulation, the elimination of one of the circuit variables (L_{lno} in (4.28)) yields a positive definite system matrix which is equivalent to the nodal circuit analysis presented in [10]. The explicit substitution of any of the circuit equations of (3.24) and (4.28) in the FE matrix part would destroy its sparsity. For the numerical example, described below, the coupled system has 47000 non-zero elements whereas the explicit Schur complement contains 1989732 non-zeros. This would destroy the efficiency of the matrix-vector product in the Krylov subspace method. Instead, a Krylov subspace solver is applied to the Schur complement without explicitly constructing the corresponding dense system of equations. The circuit matrix part is factorised in advance which is inexpensive as the circuit model typically contains only a few hundred equations. The matrix-vector product required by the Krylov subspace solver uses this factorisation within the computation of the multiplication of a vector by the Schur complement. The positive definite system is solved by CG. Since the true system matrix is not available, an algebraic preconditioner can not be constructed. However, a good preconditioner for the FE part can be used as a preconditioner for the Schur complement as well. Then, the solution process may benefit from an available powerful preconditioning technique for parabolic PDEs, such as algebraic multigrid (AMG). It should be mentioned that this preconditioner does not account for the electric behaviour of the system. As a consequence, the efficiency of this approach has to be proven experimentally for each particular model under consideration. In [11], an AMG preconditioner including the circuit equations is proposed and is shown to outperform the block preconditioning strategies presented here.

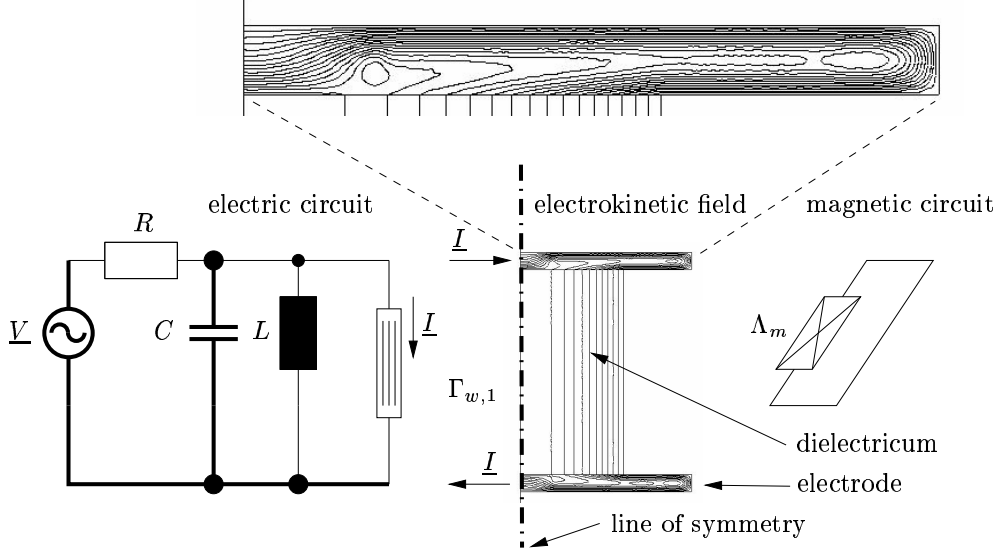


Figure 4: Axisymmetric model of a dielectric heating device: current lines in the device and in one of the electrodes.

6 Applications

The field-circuit coupling approaches are illustrated by two technical examples. The first example is a magnetic-field, electric-circuit coupled model of a 45 kW, three-phase, squirrel-cage induction machine (Fig. 1). The magnetic field in the cross-section of the machine is modelled by finite elements. The supply, the stator end windings and the rotor ring are taken into account by additional lumped parameters. The stator windings and rotor bars are represented by stranded conductor models and solid conductor models respectively. Table 1 gives the results of the topological description of the external electric circuit model. The field-circuit coupling approach enables the simulation of this hybrid model by means of a single system solution. The second example is an electrokinetic FE model combined with both an electric and a magnetic equivalent circuit, applied to a dielectric heating device (Fig. 4). A cylindrical dielectricum is placed between two circular electrodes. The magnetic equivalent circuit applies the short-circuit connection of all magnetic paths. The heating device is excited by an electric circuit containing a voltage source, a resistor and a resonant circuit. This model serves as an example both for an electrokinetic field to electric circuit coupling, which is similar to the coupling developed in Section 3, and an electrokinetic field to magnetic circuit coupling, which is similar to the coupling developed in Section 4.

7 Conclusions

The topological treatment of circuits allow for the inclusion of FE model parts. The resulting coupled systems of equations are symmetric and indefinite and are solved by Krylov subspace solvers with block preconditioning strategies. The field-circuit coupled approach offers valuable modelling facilities for electrotechnical devices.

References

- [1] L.O. Chua and P.M. Lin, *Computer Aided Analysis of Electronic Circuits - Algorithms and Computational Techniques*, Prentice-Hall, New Jersey, 1975.
- [2] H. De Gersem and K. Hameyer, “Electrodynamic finite element model coupled to a magnetic equivalent circuit,” *European Physical Journal Applied Physics*, vol. 12, no. 2, pp. 105–108, Nov. 2000.
- [3] R. Mertens, H. De Gersem, and K. Hameyer, “Transient field-circuit coupling based on a topological approach,” *COMPEL*, vol. 19, no. 2, pp. 304–309, 2000.
- [4] P. Dular, F. Henrotte, and W. Legros, “A general and natural method to define circuit relations associated with magnetic vector potential formulations,” *IEEE Transactions on Magnetics*, vol. 35, no. 3, pp. 1630–1633, May 1999.
- [5] D.A. Philips, “Coupling finite elements and magnetic networks in magnetostatics,” *International Journal for Numerical Methods in Engineering*, vol. 35, pp. 1991–2002, 1992.
- [6] J. Gyselinck, L. Vandeven, and J. Melkebeek, “Coupling finite elements and magnetic and electrical networks in magnetodynamics,” in *Proceedings of the International Conference on Electrical Machines (ICEM 98)*, Istanbul, Turkey, Sept. 1998, vol. 2, pp. 1431–1436.
- [7] I.A. Tsukerman, A. Konrad, G. Meunier, and J.C. Sabonnadière, “Coupled field-circuit problems: trends and accomplishments,” *IEEE Transactions on Magnetics*, vol. 29, no. 2, pp. 1701–1704, Mar. 1993.
- [8] C.C. Paige and M.A. Saunders, “Solution of sparse indefinite systems of linear equations,” *SIAM Journal on Numerical Analysis*, vol. 12, no. 4, pp. 617–629, 1975.
- [9] R.W. Freund, “Conjugate gradient-type methods for linear systems with complex symmetric coefficient matrices,” *SIAM Journal on Scientific Computing*, vol. 13, pp. 425–448, Jan. 1992.
- [10] J. Gyselinck and J. Melkebeek, “Numerical methods for time stepping coupled field-circuit systems,” in *Proceedings of the International Conference on Modelling and Simulation of Electric Machines, Converters and Systems (ELECTRIMACS 96)*, Saint-Nazaire, France, Sept. 1996, vol. 1, pp. 227–234.
- [11] D. Lahaye, K. Hameyer, and S. Vandewalle, “An algebraic multilevel preconditioner for field-circuit coupled problems,” in *Proceedings of the XIIIth Conference on the Computation of Electromagnetic Fields (COMPUMAG2001)*, Evian, France, July 2001, vol. 3, pp. 108–109.